ELSEVIER

Catalysis Today 81 (2003) 159–170

CATALYSIS TODAY

www.elsevier.com/locate/cattod

Kinetic study of oxidative dehydrogenation of propane over Ni-Co molybdate catalyst

M.M. Barsan, F.C. Thyrion*

Chemical Engineering Institute, Louvain University, 1 Voie Minckelers, B-1348 Louvain-la-Neuve, Belgium

Abstract

The kinetics of oxidative dehydrogenation of propane over a Ni-Co molybdate catalyst was investigated in an integral reactor by non-linear regression techniques. By performing central composite design experiments, the influence of propane and oxygen partial pressures, propane space–time and temperature were studied. A consecutive reaction network has been proposed for oxidative dehydrogenation of propane. Several possible kinetics models (power-law (PL), Mars–van Krevelen, Eley–Rideal and Langmuir–Hinshelwood) were analyzed using the statistical and thermodynamical criterions. The estimation of kinetic parameters was achieved by solving the system of ordinary differential equations, which describe the outlet of the reactor, and by minimization of the objective function using Matlab software. Data measured over the set of experimental conditions were in good agreement with two surface oxido-reduction models for the propane oxidative dehydrogenation reaction. The difference between the models consists in the surface reduction step in which one 'O' is involved for the first model, while two 'O' are required for the second model.

Keywords: Propane oxidative dehydrogenation; Nickel cobalt molybdate; Reaction kinetics; Reaction network

1. Introduction

The increasing demand of propylene, important intermediate used extensively in the petrochemical industry, has led to finding an alternative to conventional dehydrogenation process, i.e. oxidative dehydrogenation.

Unlike the dehydrogenation of propane, the oxydehydrogenation is an exothermic ΔH° (420 °C) = $-116.72\,\mathrm{kJ\,mol^{-1}}$, irreversible process ΔG° (420 °C) = $-176.09\,\mathrm{kJ\,mol^{-1}}$ [1] and eliminates the problem of frequent regeneration of catalyst to burn off the coke.

Unfortunately, the selectivity to olefins of oxidative dehydrogenation process is limited, owing to: (i) the formation of CO_x, that is thermodynamically privileged and (ii) the oxidative cleavage of propylene C=C bond. Therefore, the low selectivity toward propylene represents a problem preventing the commercial exploitation of this process. To overcome this situation in the last few years, many researches were focused on the development of selective catalyst for oxydehydrogenation of propane (ODHP). Improving the yield of propylene involves a deep understanding of the ODHP reaction mechanism. However, the publications concerning the kinetics and the mechanism of ODHP are still limited. Andersson [2] has studied the oxidation of propane over a $V/AlPO_4$ finding a Rideal type rate equation. Stern and Grasselli [3] have found that the oxidation of propane to propylene occurs via a Mars–van Krevelen mechanism, by

* Corresponding author. Tel.: +32-10-472327; fax: +32-10-472321.
E-mail address: thyrion@prcd.ucl.ac.be (F.C. Thyrion).

0920-5861/03/$ – see front matter
doi:10.1016/S0920-5861(03)00109-3

nucleophilic lattice oxygen and the deep oxidation by chemisorbed (electrophilic) oxygen. Stern and Grasselli [3] and Boisdron et al. [4] have proposed a consecutive reaction mechanism, where CO_x are produced only from further oxidation of propylene.

Creaser and Andersson [5] have investigated the ODHP over V-Mg-O considering a consecutive reaction scheme and have found that several Mars–van Krevelen type models fit the experimental data but were unable to discriminate between them. The results of Pantazidis and Mirodatos [6] and Pantazidis et al. [7] suggest a parallel reaction pathway for ODHP reaction over VMgO catalyst. Propane selective and non-selective oxidations [7] take place at the same site, involving different types of oxygen, nucleophilic lattice oxygen for the selective oxidation while adsorbed electrophilic oxygen for deep oxidation. Considering that the formation of CO_x species is due to the electrophilic oxygen (O_2, O_{2ads}, O_2^-, O^-), Pietrzyk et al. [8] have studied the ODHP on $NiMoO_4$ under transient and steady state conditions simulating those in a circulating bed reactor ("redox" mode). In spite of this research effort, many important aspects of the reaction mechanism remain unclear and therefore the factors, which control the selectivity, are far from being completely elucidated.

The aim of this work is to study the influence of the reaction variables on the propane conversion and products selectivities and to develop a kinetic model for ODHP on Ni-Co molybdate catalyst.

2. Experimental

2.1. Catalyst preparation

The nickel cobalt molybdate catalyst was prepared by co-precipitation of solutions containing stoichiometric amounts of Ni and Co nitrates and ammonia heptamolybdate. The mixed nitrate solution was added stepwise over the ammonium heptamolybdate solution, both heated at 60 °C. Using ammonium hydroxide the pH was increased and kept constant at 8.5. The solution was mixed strongly, with a constant rate, during 8 h. The temperature was maintained constant at 60 °C. The precipitate was filtered, washed with distilled water and ethanol, dried in air at 110 °C for 12 h and then it was calcined for 3 h at 500 °C in air. The catalyst was crushed and sieved in particle size of 200–250 μm.

2.2. Catalyst characterization

BET surface measurement was performed with a FlowSorb 2300 nitrogen physisorption apparatus. The BET surface area of catalyst was 95 $m^2\,g^{-1}$.

The chemical analysis of the elements was determined by ICP atomic emission spectroscopy using a Thermo Jarrell Ash Iris Advantage equipment. The sample was brought into solution by alkali oxidative fusion with $NaOH/Na_2O_2$ and subsequent dissolution with diluted HCl solution. The results of the chemical composition show a Ni/Co/Mo atomic ratio of 28.1/32.3/39.6.

X-ray diffraction (XRD) pattern was collected with a Siemens D5000 Diffractometer using Cu Kα radiation ($\lambda = 1.5418$ Å). A scan rate of 0.36° min^{-1} with a step size of 0.03° was used for data collection. The identification of the crystalline phases was realized by using references from JCPDS files [9]. The XRD pattern of the fresh sample indicates that the catalyst is a solid solution of β-$NiMoO_4$ and β-$CoMoO_4$ phases in a common molybdate lattice.

2.3. Catalytic measurements

The kinetic study was conducted at atmospheric pressure in a continuous fixed bed flow reactor. The quartz tubular reactor (internal diameter: 10 mm) was mounted vertically and surrounded by an electrically heated tubular furnace. The temperature was measured using two type K thermocouples, one positioned in the catalyst bed and the second 1 cm above. A temperature controller connected to the first thermocouple, was used to maintain constant the reaction temperature. Flow rates of gas (C_3H_8, C_3H_6, CO, O_2, He) were monitored using mass flow controllers.

The reactants and the reaction products were analyzed using two on-line gas chromatographs. Permanent gases (O_2, He, CO and CO_2) were separated using a Silica Gel 60/80 (18 ft × 1/8 in.) packed column, connected to a TCD detector. For hydrocarbons separation a Porasil B (6.6 ft × 1/8 in.) column was used coupled to a FID detector.

Conversion is defined as the molar flow of propane or oxygen transformed divided by the inlet molar flow.

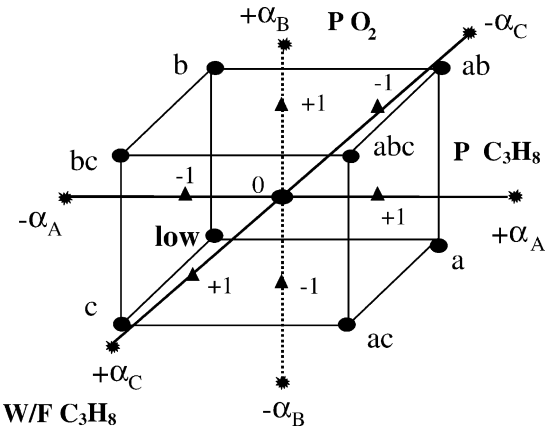

Fig. 1. Diagram of a central composite design for three factors.

Selectivity is the ratio between molar flow of product and the molar flow of consumed propane.

Preliminary tests were performed varying the catalyst particle size and gas velocity to ensure that under the chosen range of experimental conditions the mass transfer resistances could be neglected. Moreover, experiments with propane or propylene or carbon monoxide and oxygen diluted in helium, without catalyst, showed no gas-phase reaction, under the experimental conditions used in this work.

The influence of three variables, propane and oxygen partial pressures and propane space–time, over the reactants conversions and products selectivities was studied. This was realized using an experimental design with three factors called central composite design (CCD) [10]. Central composite designs are based on two level factorials and one-factor-at-a-time techniques. It allows isolating the influence of each independent variable. A modified CCD for three factors was used adding two levels noted -1 and $+1$ for each variable (Fig. 1). The choice of the values of the extreme levels, $-\alpha$ and $+\alpha$, was based on prior experimental knowledge. The value of the central level, denoted zero is the midpoint of the $-\alpha$ and $+\alpha$ values. Using mathematical formulae the values of the -1 and $+1$ levels were calculated (Table 1). Replicates of the central point were realized. Each experimental point of the CCD was performed at three temperatures: 420, 450 and 480 °C. The amounts of undiluted catalyst ($0.1 << 0.7$ g) were chosen in order to provide the propane space times given in Table 1. The

Table 1
The values of the operational variable

Variables	Notation	Levels				
		$-\alpha$	-1	0	1	$+\alpha$
$P_{C_3H_8}$ (bar)	A	0.023	0.071	0.140	0.209	0.256
P_{O_2} (bar)	B	0.015	0.043	0.084	0.124	0.152
$W/F_{C_3H_8}$ (g s μmol^{-1})	C	0.015	0.035	0.066	0.096	0.117

following procedure was used for the kinetic measurements. Starting from room temperature under the flow of reactants diluted with helium, a heating rate of 20 °C min^{-1} was supplied to reach 420 °C. After half an hour at this temperature, three analyses were automatically performed. Then the temperature was increased at a heating rate of 5 °C min^{-1} to reach first 450 °C and afterwards 480 °C and the same analysis procedure was used as at 420 °C. The analysis time at each temperature was 65 min. During the analysis period the catalyst was stable.

3. Results and discussion

3.1. Influence of oxygen partial pressure on reactants conversions and products selectivities

In order to study the influence of the oxygen partial pressure on the reaction products, the propane partial pressure and the propane space–time were kept constant at 0.14 bar and 0.066 g s μmol^{-1}, respectively while the oxygen partial pressure was varied between 0.015 and 0.152 bar. This increase in oxygen pressure increases the propane conversion (Fig. 2) from 5.4 to 20.3, while the oxygen conversion diminishes from 77.7 to 68.8% (not displayed). This enhancement in propane conversion corresponds to an increase in CO_2 selectivity of a factor of 3.2 while the selectivity to propylene decreases from 49.2 to 40.6%. The experiments performed at 450 and 480 °C (not shown) display the same increase in CO_2 selectivity when oxygen pressure increases. Therefore, a possibility to minimize the production of CO_x is to work at low partial pressure of oxygen. In the literature, a possibility to limit the formation of CO_x was envisaged by working in a membrane [11] or circulating bed reactor [8,12] in the absence of gas-phase oxygen. Indeed, it is commonly accepted that the deep oxidation

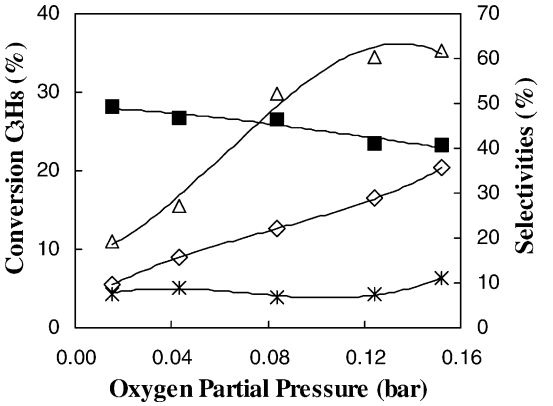

Fig. 2. Variation of propane conversion and selectivity to propylene and carbon oxides with oxygen partial pressure: (◇) propane conversion; selectivities: (■) propylene, (△) CO_2, (✳) CO. Experimental conditions: $T = 420\,^{\circ}C$, $P_{C_3H_8} = 0.14$ bar, $W/F_{C_3H_8} = 0.066\,g\,s\,\mu mol^{-1}$.

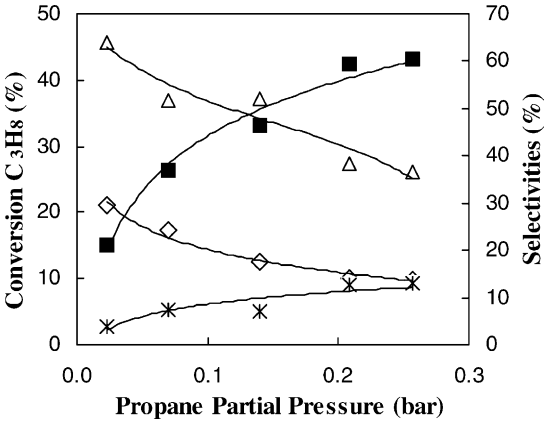

Fig. 3. Variation of propane conversion and selectivity to propylene and carbon oxides with propane partial pressure: (◇) propane conversion; selectivities: (■) propylene, (△) CO_2, (✳) CO. Experimental conditions: $T = 420\,^{\circ}C$, $P_{O_2} = 0.084$ bar, $W/F_{C_3H_8} = 0.066\,g\,s\,\mu mol^{-1}$.

engages electrophilic species O_2, O_2^-, O_2^{2-}, O^- which could be provided from the gas-phase oxygen, while the selective oxidation involves nucleophilic lattice oxygen O^{2-}.

3.2. Influence of propane partial pressure on reactants conversions and products selectivities

Several experiments were performed to understand the influence of the propane partial pressure in the feed over the performance of the catalyst, varying the partial pressure of propane between 0.023 and 0.256 bar, while the partial pressure of oxygen was fixed at 0.084 bar and propane space–time was maintained at $0.066\,g\,s\,\mu mol^{-1}$.

At 420 °C (Fig. 3), an increase of propane partial pressure of 11 times resulted in: (i) a decrease in propane conversion from 21.1 to 9.9%, (ii) a strong augmentation in oxygen conversion from 20.4 to 84.5%, (iii) an enhancement in propylene selectivity of a factor of almost 3, reaching 60.6%, (iv) a diminution in selectivity to CO_2 from 64 to 36.5% and an increase in CO selectivity by a factor of 3.5.

3.3. Influence of the propane space–time on reactants conversions and products selectivities

The effect of propane space–time on propane conversion and selectivity to the different products at 420 °C is shown in Fig. 4. To isolate the influence of propane space–time, the propane and oxygen partial pressures were kept constant at 0.14 and 0.084 bar, respectively, by simultaneous modification of propane, oxygen and helium flow rates. The propane space–time was varied from 0.015 to $0.117\,g\,s\,\mu mol^{-1}$, changing the amount of catalyst and propane flow rate. This increase of propane space–time resulted at 420 °C in: (i) an increase in propane and oxygen conversions from 6.5 to 15.1% and 24.5 to 82.2%, respectively, (ii) a

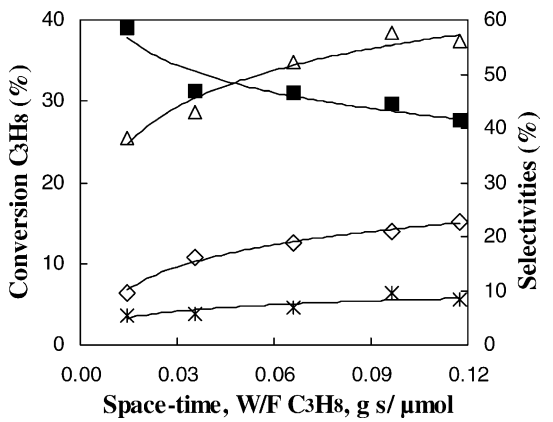

Fig. 4. Variation of propane conversion and the selectivity to each group of products with propane space–time: (◇) propane conversion; selectivities: (■) propylene, (△) CO_2, (✳) CO. Experimental conditions: $T = 420\,^{\circ}C$, $P_{C_3H_8} = 0.14$ bar, $P_{O_2} = 0.084$ bar.

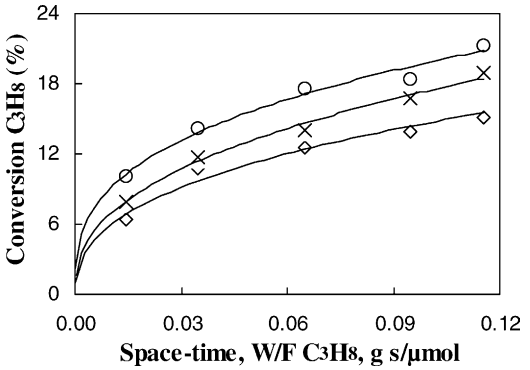

Fig. 5. Variation of propane conversion with propane space–time at all temperatures of reaction: (◇) 420 °C, (×) 450 °C and (○) 480 °C. Experimental conditions: $P_{C_3H_8} = 0.14$ bar, $P_{O_2} = 0.084$ bar.

diminution of the selectivity to propylene from 58.5 to 41.6%, (iii) an increase of the CO_2 selectivity from 38.1 to 56.1% and an augmentation in CO selectivity by a factor of 1.5. Fig. 5 reports a similar behavior for the propane conversion against propane space–time at different temperatures.

3.4. Reaction network

The results of the catalytic tests during the ODHP over Ni-Co molybdate show that the main products are propylene, carbon dioxide and carbon monoxide. In addition, traces of methane and ethylene are also produced. No oxygenated products (aldehydes, acids) were detected. Taking into account the above observations the following set of reactions was proposed.

Oxidative dehydrogenation of propane to propylene:

$$C_3H_8 + 0.5O_2 = C_3H_6 + H_2O \quad (1)$$

Oxidation of propane to carbon dioxide and monoxide:

$$C_3H_8 + 5O_2 = 3CO_2 + 4H_2O \quad (2)$$

$$C_3H_8 + 3.5O_2 = 3CO + 4H_2O \quad (3)$$

Oxidation of propylene to carbon dioxide and monoxide:

$$C_3H_6 + 4.5O_2 = 3CO_2 + 3H_2O \quad (4)$$

$$C_3H_6 + 3O_2 = 3CO + 3H_2O \quad (5)$$

Oxidation of carbon monoxide:

$$CO + 0.5O_2 = CO_2 \quad (6)$$

Cracking of propane:

$$C_3H_8 = CH_4 + C_2H_4 \quad (7)$$

A possibility to distinguish the main features of a reaction network is by analyzing the behavior of the products yields as a function of the reactant conversion. It can be observed from Fig. 6 that the propylene yield increases with propane conversion reaching a maximum value clearly visible at the highest temperatures, and then it decreases due to the consecutive transformation into CO_x products. In addition, the selectivity to carbon oxides (Fig. 4) increases with space–time behavior typical of secondary products. Therefore, the experimental results suggest a consecutive reaction pathway.

Some additional experiments were carried out using CO or propylene or a mixture propane/propylene instead of propane as feed.

To obtain new information concerning the oxidation of CO, Eq. (6), a mixture of CO/O_2/He in the same proportion as point $-\alpha_A$ was used. The CO conversion obtained at 420 °C was 60% and linearly increased with the temperature, reaching 71.4 and 80.7% at 450 and 480 °C, respectively. The amount of CO used as feed in this experiment is higher than the maximum quantity of CO resulting from the ODHP under the reaction conditions. This result allows confirming that most of the CO formed during the ODHP reaction over Ni-Co molybdate is transformed in CO_2.

To achieve additional insights into the subsequent mechanism the oxidation of propylene was studied under experimental conditions corresponding to $-\alpha_A$ (excess of oxygen) and zero (excess of propylene) levels. The results were compared with those obtained when propane was used as feed (Fig. 7). Under the same conditions of reaction, at 450 °C the conversion of propane alone (26.8% for $-\alpha_A$ and 14.1% for zero levels) is a little bit higher than the one of propylene alone (23.6 and 11.6%). This was a surprising result because it was expected that the propylene conversion should be the highest due to the reactivity of the double bond.

Propane and propylene were also fed together (molar ratio 1:1), under the experimental conditions corresponding to $-\alpha_A$ and zero levels, reducing the

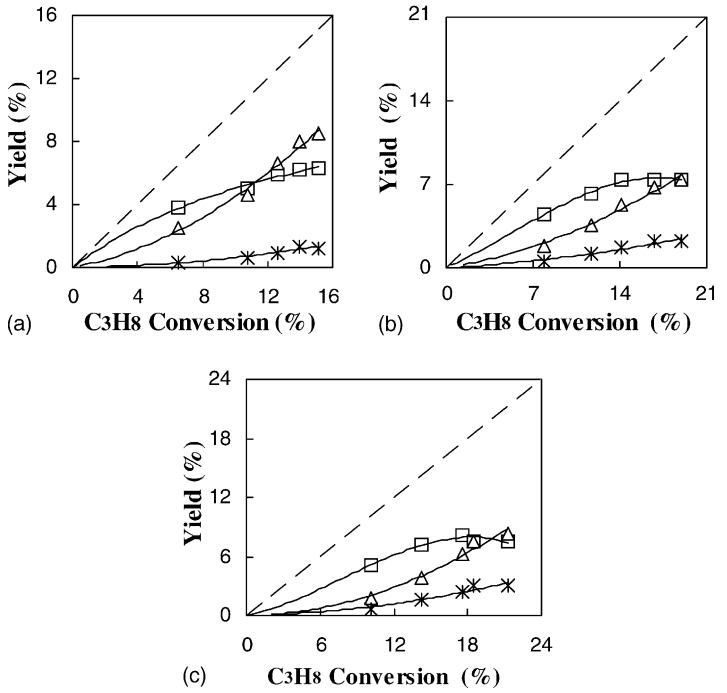

Fig. 6. Variation of the yield of propylene and CO_x with propane conversion at all reaction temperatures: (a) 420 °C, (b) 450 °C and (c) 480 °C; yields: (□) propylene, (△) CO_2, (✳) CO.

amount of helium with the added amount of hydrocarbon. In this manner, the partial pressures of oxygen, propane and propylene remained the same as in the separated experiments, when only one hydrocarbon was used. At the experimental point $-\alpha_A$ (excess of oxygen) the conversion of propane decreases very strongly from 26.8 to 3.7%, while the propylene conversion decreases only from 23.6 to 18.5%, when the two hydrocarbons were cofed. Changing the experimental conditions at zero level (excess of hydrocarbons), the same behavior for hydrocarbon conversions was observed. The conversion of propane diminishes from 14.1 to 0% consequently when propylene is cofed. These decreases in hydrocarbon conversions are consistent with the competition between propane and propylene for the same catalytic sites. The above data reveal that the decrease of the propane conversion is much higher than the decrease of propylene conversion, which lead us to the conclusion that the propylene competes more effectively than propane for the same adsorption sites.

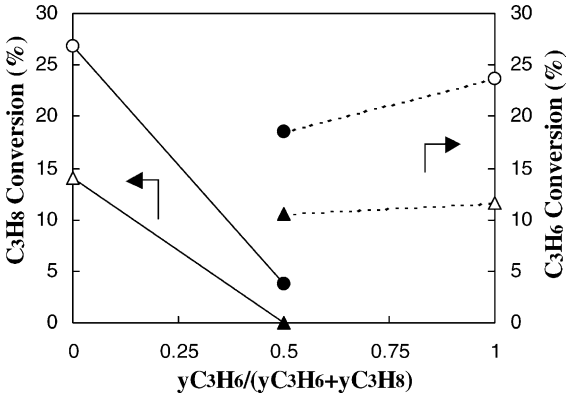

Fig. 7. Variation of hydrocarbons (HC) conversion with the fraction of propylene in the hydrocarbons mixture. Experimental conditions corresponding to $-\alpha_A$ (○), e.g. P_{HC}/P_{O_2} 0.023/0.084, zero level (△), i.e. P_{HC}/P_{O_2} 0.14/0.084, (●) P_{HC}/P_{O_2} 0.046/0.084, (▲) P_{HC}/P_{O_2} 0.28/0.084, $T = 450$ °C.

3.5. Kinetic modeling

The kinetic parameters were determined by fitting the gas-phase composition measured at the outlet of

the reactor with several rate equations by non-linear regression.

By analyzing the above set of reactions (1)–(7), it can be observed that not all reactions are linearly independents. For instance, Eq. (2) is a linear combination of Eqs. (3) and (6), Eq. (4) can be obtained from Eqs. (5) and (6), while Eq. (3) is obtained by adding Eq. (1) at Eq. (5). In consequence, the dependent Eqs. (2)–(4) are not considered in the modeling process. The intensive extent of reaction, ξ_m, was calculated for each independent reaction. The value of ξ_m obtained for the propane cracking reaction (7) was much smaller than the one obtained for the other independent reactions. Therefore, Eq. (7) was eliminated from the reaction network and the following simplified scheme was considered:

$$C_3H_8 \underset{r_1(\xi_{m_1})}{\rightarrow} C_3H_6 \underset{r_2(\xi_{m_2})}{\rightarrow} CO \underset{r_3(\xi_{m_3})}{\rightarrow} CO_2$$

where $r_i(\xi_{m_i})$ is the rate of reaction i expressed in function of intensive extent of reaction, ξ_m.

The evolution of the composition of the reaction mixture along the axial coordinate z of the plug flow reactor is calculated by a system of differential equations of mass balance, where the number of equations is equal to the number of stoichiometric independent reactions:

$$\frac{d\xi_{m_i}}{dz} = \frac{S\rho_{bed}}{\dot{m}} r_i(\xi_{m_1}, \xi_{m_2}, \ldots, \xi_{m_r}), \quad i = 1, 2, \ldots, r \tag{8}$$

In Eq. (8), the following notations were used: $\dot{m}$ is total mass flow rate, S cross-section area of the reactor, ρ_{bed} the density of the catalytic bed.

The initial conditions of this system are:

$$z = 0, \quad \xi_{m_i} = 0, \quad i = 1, \ldots, r \tag{9}$$

The resulting system of the ordinary differential equations was solved using Matlab function ODE23( ), based on a Runge–Kutta (2, 3) pair method of Bogacki and Shampire. The objective function was the minimization of the sum of squares of the difference between the experimental and calculated value for intensive extent of reaction:

$$OF = \sum_{l=1}^{n}\sum_{i=1}^{r}[(\xi_{m_{il}})_{Exp} - (\xi_{m_{il}})_{Calc}]^2 \tag{10}$$

where n is the number of experiments.

The optimization of the rate parameters was achieved according to a large-scale algorithm based on the interior-reflective Newton method. In the calculation, the model is evaluated at each reaction temperature to obtain a set of parameters. The physico-chemical meaning of the resulting parameters is verified using the Arrhenius and/or Van't Hoff laws [13,14]. The activation energies, Ea_i, and the adsorption enthalpies, ΔH, were determined by the equations:

$$k_i = k_{0,i} \exp\left(-\frac{Ea_i}{RT}\right) \tag{11}$$

$$K = K_0 \exp\left(\frac{\Delta H}{RT}\right) \tag{12}$$

The adequacy of the fitted models was checked by examining the residual sum of square, the parity plots and by performing an approximate lack of fit test (F-test). Concerning the significance of the estimated kinetic parameters, the individual 95% confidence intervals have been calculated.

3.6. Kinetic models

Several rate expressions based on mechanistic models were selected for the reaction of propane oxidation to propylene (Table 2). For the transformation of propylene into CO and the subsequent oxidation into CO_2, the following power-law (PL) models were chosen:

$$r_2 = k_2 P_{C_3H_6}^{m_2} P_{O_2}^{n_2} \tag{13}$$

$$r_3 = k_3 P_{CO}^{m_3} P_{O_2}^{n_3} \tag{14}$$

The reaction mechanisms giving rise to the reaction rates of propane oxidation in propylene can be grouped in three main types:

(a) Langmuir–Hinshelwood type mechanism, which assumes that the rate determining step is the reaction between two adsorbed reactants. Model 1 supposes that the adsorption of propane and molecular oxygen occurs on the same catalytic sites (competitive adsorption). Models 2 and 3 presume the adsorption of reactants on different sites (non-competitive adsorption) with non-dissociative oxygen adsorption for Model 2 and dissociative oxygen adsorption for Model 3.

Table 2
Rate equations considered for propane oxidation to propylene

Type of model	Rate expression
Langmuir–Hinshelwood	
1	$r = \frac{k_{LH} K_{O_2} K_{C_3H_8} P_{O_2} P_{C_3H_8}}{(1 + K_{O_2} P_{O_2} + K_{C_3H_8} P_{C_3H_8})^2}$
2	$r = \frac{k_{LH} K_{O_2} K_{C_3H_8} P_{O_2} P_{C_3H_8}}{(1 + K_{O_2} P_{O_2})(1 + K_{C_3H_8} P_{C_3H_8})}$
3	$r = \frac{k_{LH} K_{C_3H_8} P_{C_3H_8} \sqrt{K_{O_2} P_{O_2}}}{(1 + \sqrt{K_{O_2} P_{O_2}})(1 + K_{C_3H_8} P_{C_3H_8})}$
Eley–Rideal	
4	$r = \frac{k_{ER} K_{O_2} P_{O_2} P_{C_3H_8}}{1 + K_{O_2} P_{O_2}}$
5	$r = \frac{k_{ER} K_{O_2} P_{O_2} P_{C_3H_8}}{(1 + K_{O_2} P_{O_2})^2}$
6	$r = \frac{k_{ER} P_{C_3H_8} \sqrt{K_{O_2} P_{O_2}}}{1 + \sqrt{K_{O_2} P_{O_2}}}$
Surface oxido-reduction (SOR)	
7	$r = \frac{k_{O_2} k_{C_3H_8} (P_{O_2})^n P_{C_3H_8}}{k_{O_2} (P_{O_2})^n + \nu k_{C_3H_8} P_{C_3H_8}}, \; n = 0.5$
8	$r = \frac{k_{O_2} k_{C_3H_8} (P_{O_2})^n P_{C_3H_8}}{k_{O_2} (P_{O_2})^n + \nu k_{C_3H_8} P_{C_3H_8}}, \; n = 1$
9	$r = \frac{1}{\nu} k_{O_2} P_{O_2} \left[1 + \frac{k_{O_2}}{2\nu k_{C_3H_8}} \frac{P_{O_2}}{P_{C_3H_8}} - \sqrt{\left(\frac{k_{O_2}}{2\nu k_{C_3H_8}} \frac{P_{O_2}}{P_{C_3H_8}} \right)^2 + \frac{k_{O_2}}{\nu k_{C_3H_8}} \frac{P_{O_2}}{P_{C_3H_8}}} \right]$
10	$r = \frac{k_{O_2} k_{C_3H_8} P_{O_2} P_{C_3H_8}}{k_{O_2} P_{O_2} + \nu k_{C_3H_8} P_{C_3H_8}} \left(1 - \frac{k_{O_2}}{k'_{O_2}} P_{O_2} \right)$
11	$r = \frac{k_{O_2} k_{C_3H_8} P_{O_2} P_{C_3H_8}}{k_{O_2} P_{O_2} + \nu k_{C_3H_8} P_{C_3H_8} + (k_{O_2} k_{C_3H_8} / k_P) P_{O_2} P_{C_3H_8}}$

(b) Eley–Rideal type mechanism, which considers as the rate-determining step, the reaction between propane in the gas-phase and adsorbed oxygen. Models 4 and 5 suppose the non-dissociative oxygen adsorption, while Model 6 assumes the dissociative oxygen adsorption. Model 5 considers two adjacent sites.
(c) Contrary to the Langmuir–Hinshelwood and Eley–Rideal models, which suppose one rate controlling step, the models denoted hereafter SOR [15] consider two or three rate-controlling steps.

Models 7 and 8 are classical Mars–van Krevelen models, which suppose that the rate of reduction of the catalyst by propane is equal to the rate of oxidation. Model 9 is an alternative to Model 8, involving the interaction of propane with two 'O' species. The same equality between the rate of reduction and the rate of oxidation is considered. Models 10 and 11 consider the equality of the three rates of the elementary steps. Model 10 assumes that the rate of reduction of the catalyst, the rate of oxygen chemisorption and the rate of dissociation of adsorbed oxygen are equal. Model 11 supposes that the adsorbed reaction product is slowly desorbed and occupies a substantial part of the catalyst surface. In this case, the rate of reduction of the catalyst is equal to the rate of oxidation and to the rate of the product desorption.

The analysis of the results obtained by fitting the experimental data with the above rate equations leads to the conclusion that the residual sum of squares obtained for Langmuir–Hinshelwood-PL models was higher than the one obtained for the SOR-PL models with the same number of parameters. Regarding the physico-chemical meaning of the kinetic parameters, it was found that the estimated adsorption constants of propane and oxygen do not respect the Van't Hoff law. For these reasons, the Langmuir–Hinshelwood-PL models were rejected.

The models Eley–Rideal-PL show a residual sum of squares higher than the SOR-PL models, with the same number of parameters. For instance, the residual sum of squares obtained at 420 °C for Eley–Rideal Model 4-PL is 2.95×10^{-3} while for SOR Model 8-PL is 9.38×10^{-4}. In addition, one or more kinetic parameters do not respect the Arrhenius and Van't Hoff laws. Taking into account these results, the Eley–Rideal-PL models were also rejected as being inadequate for the studied process.

Concerning the SOR-PL models, it can be observed that they are the most adequate, among the fitted models, with respect to the residual sum of squares. Model 7-PL, which is a Mars–van Krevelen type with 0.5 order oxygen dependence for ODHP, was rejected due to its highest residual sum of squares. Model 11-PL was also eliminated for the same reason. Model 9-PL presents the lowest residual sum of squares at all reaction temperatures, followed by Models 8-PL and 10-PL (Table 3). The values for residual sum of squares for Models 8-PL and 10-PL are very close, especially at 450 and 480 °C, but taking into account the principle of parsimony, the model with the lesser number of parameters is preferred. In addition, $k'_{O_2} \gg k_{O_2}$ so the term $k_{O_2} P_{O_2} / k'_{O_2} \rightarrow 0$ and Model 10 can be reduced to Model 8. Further experiments will be necessary to discriminate between these two models (Models 8 and 9). However, it is obvious from the above results that a surface oxido-reduction type model better describes the experimental results obtained for the ODHP reaction. Fig. 8 shows the parity plots of propane, oxygen conversions as well as the selectivities in propylene, carbon dioxide obtained with Model 9-PL using the kinetic parameters reported in Table 4. The orders with respect to oxygen determined in Eqs. (13) and (14) are both first-order while they are zero order in propylene and carbon monoxide respectively. A possible explanation of the above results could be that the catalyst surface is saturated with propylene and carbon monoxide (catalyst reduced). In addition, the most important part of experiments was conducted in excess of propane, so oxygen becomes a limitative reactant, which explains the important dependence of oxygen.

Taking into account the results of simulation, where two models of surface oxido-reduction type are the most probable (Models 9-PL and 8-PL), the following reaction mechanism is proposed. For both models, the step of re-oxidation of the surface is described by Eqs. (15a) and (15b). The difference between the two models consists in the reduction step where one 'O' is involved in Model 8, Eq. (16) and two 'O' in Model 9, Eq. (17).

Surface oxidation:

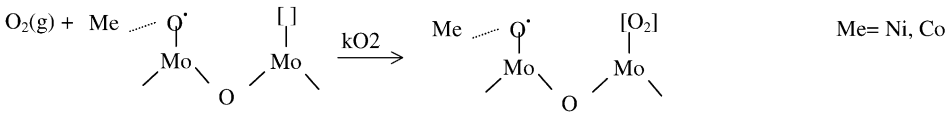

(15a)

Table 3
Comparison of the different SOR-PL models with respect the residual sum of squares obtained

Model	Number of parameters	Residuals sum of squares			Comments
		420 °C	450 °C	480 °C	
Model 7-PL	8	2.0995×10^{-3}	1.2353×10^{-3}	1.5110×10^{-3}	Rejected
Model 8-PL	8	9.3800×10^{-4}	1.0900×10^{-3}	8.4500×10^{-4}	Retained
Model 9-PL	8	8.1023×10^{-4}	1.0605×10^{-3}	8.1872×10^{-4}	Retained
Model 10-PL	9	9.8617×10^{-4}	1.0874×10^{-3}	8.3810×10^{-4}	Retained
Model 11-PL	9	1.9196×10^{-3}	1.2081×10^{-3}	1.4400×10^{-3}	Rejected

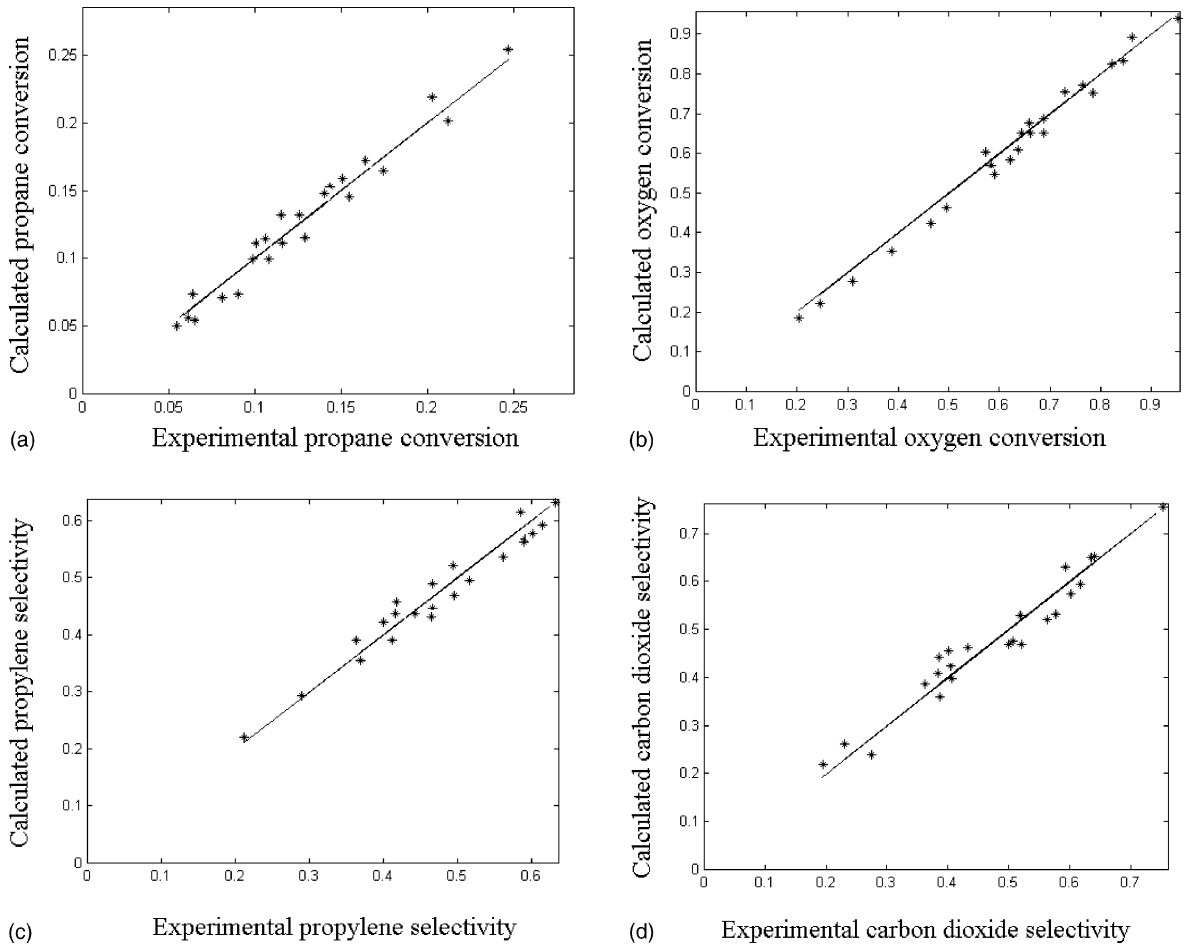

Fig. 8. Comparison of experimental and calculated values of (a) propane conversion, (b) oxygen conversion, (c) selectivity to propylene and (d) selectivity to CO_2 at 420 °C (using Model 9-PL and parameters of Table 4).

Table 4
Kinetic parameters of Model 9-PL

k_0	Value	Units	Ea (kJ mol^{-1})
k_{0,O_2}	$7.618 \times 10^3 \pm 0.4 \times 10^3$	mol kg^{-1} s^{-1} bar^{-1}	73.43 ± 4.8
k_{0,C_3H_8}	$1.810 \times 10^5 \pm 0.13 \times 10^5$	mol kg^{-1} s^{-1} bar^{-1}	80.10 ± 10.2
$k_{0,2}$	$2.621 \times 10^4 \pm 0.12 \times 10^4$	mol kg^{-1} s^{-1} bar$^{-(m_2+n_2)}$	83.31 ± 8.6
$k_{0,3}$	3.781 ± 0.21	mol kg^{-1} s^{-1} bar$^{-(m_3+n_3)}$	25.63 ± 1.2

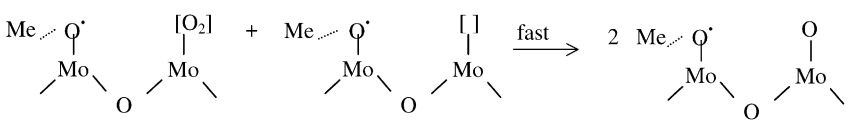

(15b)

Surface reduction:

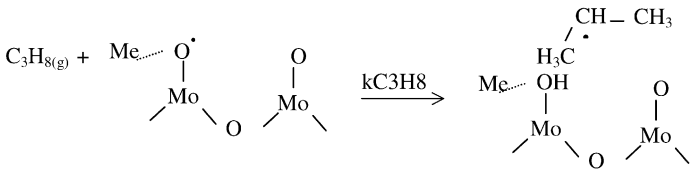

(16)

or

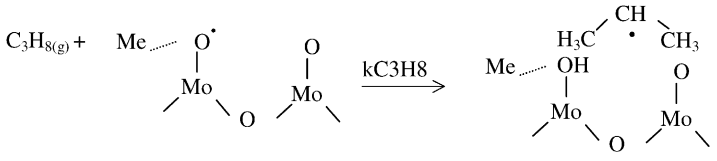

(17)

(18)

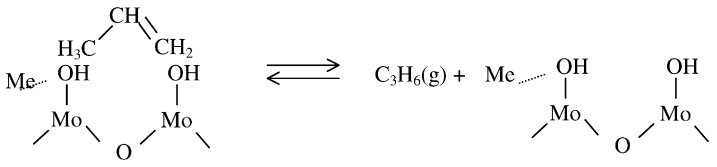

(19)

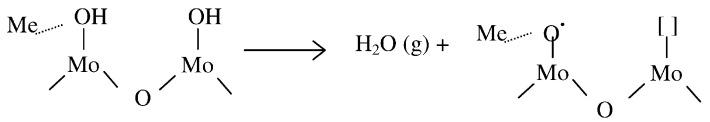

(20)

$$C_3H_{6(ads)} + 3(x+2)[O] \rightarrow 3CO_{x(g)} + 6OH_{(ads)} \quad (21)$$

For both models, an adsorbed propyl radical issued from propane by an initial hydrogen abstraction is considered the reaction intermediate [16]. This propyl radical is subsequently transformed by a second hydrogen abstraction into adsorbed propylene and an OH group, Eq. (18). One part of adsorbed propylene desorbs in the gas-phase and the other remains adsorbed at the surface and forms carbon oxides.

Further kinetic modeling is in progress based on these proposed mechanisms of ODHP reaction over Ni-Co molybdate.

4. Conclusions

The kinetic of ODHP reaction was studied over the Ni-Co molybdate catalyst under steady-state conditions in a classical fixed bed reactor. A consecutive reaction network was proposed for ODHP, in which the propylene is produced by the oxidation of propane, while carbon monoxide is produced by the successive oxidation of propylene and carbon dioxide by the further oxidation of carbon oxide.

For the main reaction, ODHP, several mechanistic models were considered (LHHW, ER and SOR

models), while for the other two reactions, PL models were selected.

The results show that two surface oxido-reduction models (Models 8 and 9) were the most suitable for ODHP. The differences between the residual sums of squares determined for these two models are very small, so further experiments are necessary to discriminate among them. Model 8 is a classical Mars–van Krevelen, in which the rate of the surface re-oxidation step is equal with the rate of the surface reduction step. The former step involves the reaction of propane with one 'O' leading to the formation of an intermediate, which is then converted, into reaction product, propylene. From the point of view of the reaction mechanism, the step of surface re-oxidation is identical for both selected models; the difference between the models consists in the surface reduction step in which one 'O' is involved for Model 8, while two 'O' [17] are necessary in case of Model 9.

In addition, it was demonstrated that propane and propylene compete for the same adsorption sites, propylene competing more effectively than propane.

Acknowledgements

The financially support of the Région Wallonne (Belgium) in the frame of an 'Action de Recherche Concertée' is gratefully acknowledged.

References

[1] C.L. Yaws, P.-Y. Chiang, Hydrocarbon Process. 11 (1988) 81.
[2] S.L.T. Andersson, Appl. Catal. A 112 (1994) 209.
[3] D.L. Stern, R.K. Grasselli, J. Catal. 167 (1997) 560.
[4] N. Boisdron, A. Monnier, L. Jalowiecki-Duhamel, Y. Barbaux, J. Chem. Soc. Faraday Trans. 91 (17) (1995) 2899.
[5] D. Creaser, B. Andersson, Appl. Catal. A 141 (1996) 131.
[6] A. Pantazidis, C. Mirodatos, in: Proceedings of the 11th International Congress on Catalysis—40th Anniversary, Stud. Surf. Sci. Catal. 101 (1996) 1029.
[7] A. Pantazidis, S.A. Bucholz, H.W. Zanthooff, Y. Schuurman, C. Mirodatos, Catal. Today 40 (1998) 207.
[8] S. Pietrzyk, M.L. Ould Mohamed Mahmoud, T. Rembeczky, R. Bechara, M. Czernicki, N. Fatah, Stud. Surf. Sci. Catal. 109 (1997) 263.
[9] JCPDS Powder Diffraction File, International Centre for Diffraction Data, PA, 1999.
[10] T.B. Barker, Quality by Experimental Design, Marcel Dekker, New York, 1985.
[11] G. Capannelli, E. Carosini, F. Cavani, O. Monticelli, F. Trifiro, Chem. Eng. Sci. 51 (1996) 1817.
[12] F. Genser, S. Pietrzyk, Chem. Eng. Sci. 54 (1999) 4315.
[13] G.F. Froment, K.B. Bischoff, Chemical Reactor Analysis and Design, second ed., Wiley, New York, 1990.
[14] G.F. Froment, L.H. Hosten, Catalysis: Science and Technology, vol. 2, Springer, Berlin, 1981, pp. 97–170.
[15] G.I. Golodets, Heterogeneous Catalytic Reactions Involving Molecular Oxygen, Stud. Surf. Sci. Catal., vol. 15, Elsevier, Amsterdam, 1983.
[16] D.L. Stern, R.K. Grasselli, Stud. Surf. Sci. Catal. 110 (1997) 357.
[17] M.D. Argyle, K. Chen, C. Ressini, A.T. Bell, E. Iglesia, 223 National Meeting, ACS, 2002 (oral presentation).